

EMPIRICAL-BASED INFILL MODEL ACCOUNTING FOR IN-PLANE/OUT-OF-PLANE INTERACTION APPLIED FOR THE SEISMIC ASSESSMENT OF EC8-DESIGNED RC FRAMES

Paolo Ricci¹, Mariano Di Domenico¹, Gerardo M. Verderame¹

¹ University of Naples Federico II
Department of Structures for Engineering and Architecture
Via Claudio 21 – 80125 – Naples – Italy
{paolo.ricci, mariano.didomenico, verderam}@unina.it

Keywords: URM infill wall, out-of-plane, incremental dynamic analyses, seismic assessment, in-plane/out-of-plane interaction, macro-model.

Abstract. *In the Mediterranean area, Reinforced Concrete (RC) buildings are usually provided of Unreinforced Masonry (URM) infill wall panels. When subjected to seismic action, these non-structural elements are sensitive to the displacements produced in the In Plane (IP) direction and to the acceleration in the Out Of Plane (OOP) direction. The damage due to IP displacements reduce the OOP capacity and vice-versa: this phenomenon is called IP-OOP interaction. Proposed empirical-based formulations both for predicting infills OOP strength and for modeling the effects of IP displacement demand on OOP behavior and vice versa are illustrated. A new lumped-plasticity macro-model based on the proposed empirical formulations and conceived to represent the IP and the OOP behavior taking into account the mutual interaction effects is defined. Part of the proposed modelling strategy is a routine that removes the whole infill panel from the structural model in case of its IP or OOP collapse. In this paper, the proposed model is described and applied to model the infills of case-study infilled RC frames designed according to Eurocode 8 and different for design PGA at Life Safety Limit State. The results of non-linear time-history analyses are presented and discussed in order to show the effects of taking into account or neglecting the IP-OOP interaction phenomena in assessing the seismic response of the case-study buildings.*

1 INTRODUCTION

In the Mediterranean area, Reinforced Concrete (RC) buildings are usually provided of Unreinforced Masonry (URM) infill wall panels. When subjected to the seismic action, these non-structural elements are sensitive to the displacements produced in the In Plane (IP) direction and to the acceleration in the Out Of Plane (OOP) direction [1]. IP displacements can damage infill walls and produce the attainment of the Damage Limitation Limit State (DL), with significant effects in terms of repairing costs for RC buildings after earthquakes. OOP acceleration can produce infills' collapse by their overturning, which is a great risk for life safety as well as an obstacle to escape/rescue operations during seismic emergency [2]: in this sense, the OOP collapse of infill walls is associable to the attainment of the Life Safety Limit State (LS). A great number of experimental and analytical works concerning the IP behaviour of URM infills is available in literature ([3-6], among many others) and some analytical and experimental works have been proposed about their OOP behaviour, especially in recent years ([7-15], among others), and concerning the IP-OOP interaction phenomena, i.e., the effects of IP actions on the OOP behaviour and vice versa. For instance, several authors showed through analytical and experimental studies how the IP displacement demand affects the OOP response of infills in terms of capacity and demand acting on them.

In this work, a state of art concerning URM infills modelling strategies accounting for their OOP behaviour and the IP-OOP interaction is reported. An empirical-based URM infill macro-model accounting for the IP-OOP interaction implemented in OpenSEES is introduced. Then, two case study RC buildings designed in accordance with Eurocodes 2 and 8 recommendations, different for design PGA at LS (0.15 and 0.35 g), are described. The case-study bare frames are infilled with a single-wythe thick and strong infill wall. Incremental Dynamic Analyses (IDAs) are carried out on the infilled case-study buildings in order to define in a non-linear incremental framework the different seismic capacity assessed with and without accounting for the IP-OOP interaction phenomena.

2 STATE OF ART

In [16] Hashemi and Mosalam proposed a strut and tie macro-model of infills based on the results of FEM analyses. In this model, the infill is represented by eight no-tension truss elements joined in the center by a no-compression truss element. Mechanical and geometric characteristics of struts and tie are calibrated in order to obtain an interaction domain of IP OOP action which follows the one obtained through FEM analyses.

In [11] Kadysiewski and Mosalam introduced a macro-model in which the infill is modelled through one diagonal beam element pinned at the edges provided of a lumped mass in the center active only in the OOP direction. The OOP behaviour is assumed as elastic-plastic. To account for the IP-OOP interaction, the authors introduce interaction domains in terms of yielding force and collapse displacements derived from numerical analyses. Integral part of the discussed model is a routine that removes from the structural model the elements representative of the infill when their IP-OOP displacement history exceeds the convex interaction domain in terms of ultimate displacement.

Furtado et al. [17] defined a "Kadysiewski and Mosalam-based" macro-model in which the infill is represented by 4 diagonal rigid elements joined in the center by one element which takes into account the non-linearity of the infill behaviour. The central element is joined to the diagonal struts through 2 nodes in which the OOP mass is lumped. Also in this case, part of the model is an algorithm that removes the elements representative of the infill from the structural model if its IP-OOP displacement history exceeds a linear interaction domain in terms of ultimate displacement. A macro-model based on the one defined by Kadysiewski and Mosalam-

am was also proposed by Longo et al. [18]. Shing et al. [19] proposed a macro-model in which the infill wall is represented by two fiber-section diagonals accounting for the IP-OOP interaction and through a vertical and a horizontal element accounting for the bi-directional arching action.

An infill wall model accounting for the IP-OOP interaction was proposed by Oliaee and Magenes [20]. The infill is represented by 2 diagonals, each one divided into 2 non-interacting in-series no-tension elements, an inelastic truss representing IP behaviour and a distributed inelasticity fiber element representing OOP behaviour. The IP-OOP interaction is introduced through the updating of the strain at peak load of the material assigned to fibers (OOP stiffness reduction) and through the reduction of the fiber elements' thickness (OOP strength reduction) depending on the maximum IP displacement registered.

3 EMPIRICAL-BASED URM INFILL MODEL ACCOUNTING FOR IP-OOP INTERACTION

Experimental tests aimed at assessing the OOP behaviour of URM infills and the effects of IP displacement demand on the OOP capacity were performed by different authors ([7-15], among others). In a companion paper [21], the Authors of this study collected in a database the values of secant stiffness and lateral force registered for the above test specimens at first macro-cracking and peak load, as well as the value, if provided, of their ultimate OOP displacement. The application of code and literature provisions aimed at predicting stiffness, force and displacement associated to the significant points of the OOP backbone of URM infills showed that:

- 1) Timoshenko's formula [22] for the calculation of the lateral stiffness of an elastic isotropic plate provides a good estimation of URM infills secant stiffness at first macro-cracking point (Equation 1).

$$K_{crack} = \frac{bD}{\alpha a^3} \quad (1)$$

In Eq. 1, a and b are the shorter and longer dimensions of the infill, respectively, while D is the plate flexural stiffness and α is a parameter accounting for the infill aspect-ratio and boundary conditions.

- 2) Dawe and Seah's [9] formulation accounting for two-way arching action exhibits good performances in predicting the OOP strength of URM infills, as well as Kadysiewski and Mosalam approach [11] based on the first vibration frequency of a distributed-mass cracked beam pinned at edges produces good predictions of their secant stiffness at peak load (Equation 2).

$$K_{max} = 6.562E \frac{w}{(h/t)^3} \quad (2)$$

In Eq. 2, E is the infill elastic modulus in the vertical direction, w , h and t are the infill width, height and thickness, respectively.

- 3) No literature or code provision is applicable to obtain a good prediction of URM infills OOP collapse displacement.

In order to define a tri-linear OOP backbone for infills, in an empirical-based framework, a least square linear regression was carried out on the experimental uniformly distributed first cracking loads, q_{crack} , reported in the collected database. Moreover, to obtain a more reliable prediction of the uniformly distributed peak load, q_{max} , with respect to the one provided by

applying Dawe and Seah's relationship, a least square linear regression was carried out on the experimental values of q_{\max} , too. The obtained relationships are:

$$q_{\text{crack}} = 0.31 f'_m{}^{0.05} \frac{t}{h^{2.66}} \quad (3)$$

$$q_{\max} = 1.95 f'_m{}^{0.35} \frac{t^{1.59}}{h^{2.96}} \quad (4)$$

K_{crack} and K_{\max} should be calculated by applying equations (1) and (2), respectively.

Based on experimental evidences (Angel et al. [8], Guidi et al. [14], Calvi and Bolognini [13], Griffith and Vaculik [12]), a plastic post-peak behaviour is assumed and the collapse OOP displacement is assumed equal to 3.7 times the predicted displacement at peak load.

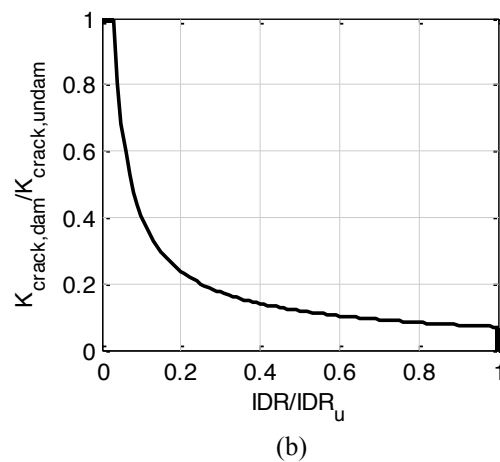
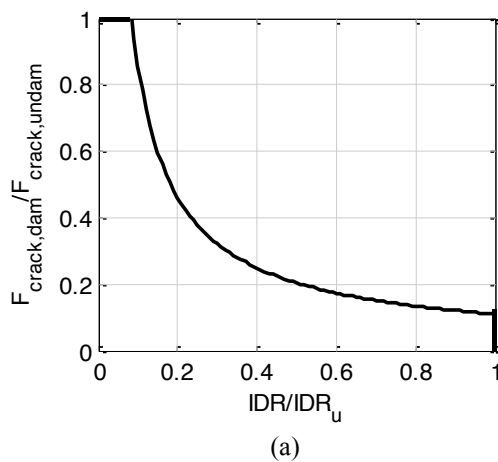
Based on experimental evidences, relationships aimed at predicting secant stiffness and lateral strength at first cracking and peak load degradation due to IP damage represented by the maximum IDR attained during the IP loading normalized with respect to the IDR corresponding to the complete loss of IP loads bearing capacity by the infill, IDR_u , were defined.

$$\frac{P_{\text{dam}}}{P_{\text{undam}}} = \begin{cases} \min \left\{ 1 ; \alpha \left(\frac{IDR}{IDR_u} \right)^\beta \right\} & \text{if } IDR < IDR_u \\ 0 & \text{if } IDR \geq IDR_u \end{cases} \quad (5)$$

In Eq. 5, P_{dam} is the observed variable for the infill that underwent a maximum IP displacement represented by the IDR, P_{undam} is the same observed variable for the undamaged infill, and the α and β coefficients are determined through a linear least squares regression in the log-log plan (Table 1). Clearly, $P_{\text{dam}}/P_{\text{undam}}$ cannot be higher than 1 and must be equal to 0 if $IDR \geq IDR_u$, i.e., the OOP capacity drops to zero at the infill IP collapse, as shown in Figure 1.

	$K_{\text{crack,dam}}/K_{\text{crack,undam}}$	$F_{\text{crack,dam}}/F_{\text{crack,undam}}$	$K_{\text{max,dam}}/K_{\text{max,undam}}$	$F_{\text{max,dam}}/F_{\text{max,undam}}$
α	0.07	0.11	0.12	0.27
β	-0.76	0.89	-0.69	-0.37

Table 1. α and β values for Equation 5.



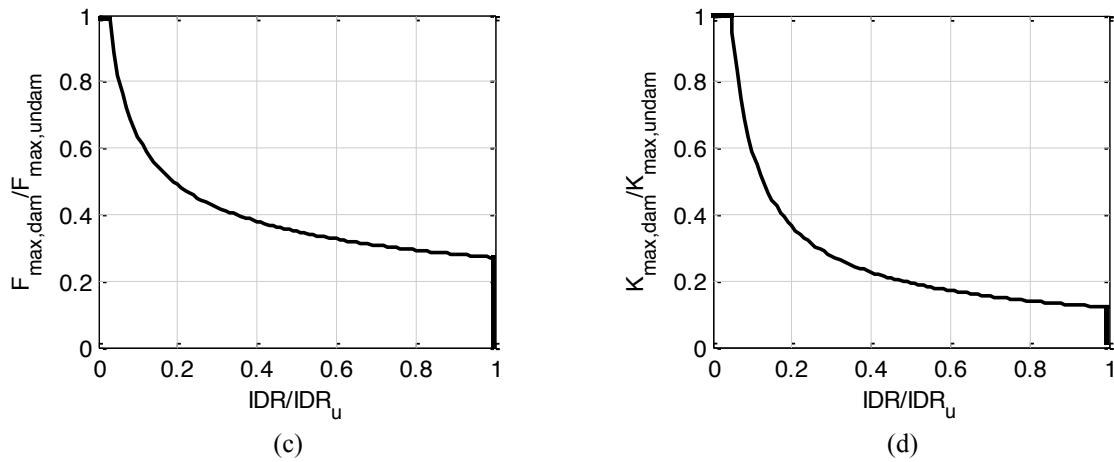


Figure 1. Degradation of first macro-cracking force (a) and secant stiffness (b) and of peak load force (c) and secant stiffness (d) due to IP damage represented by the current IDR normalized with respect to IP collapse IDR, IDR_u .

Based on the only reliable experimental datum provided on this issue in literature by Furtado et al. [15], it is assumed that the $d_{u,dam}/d_{u,undam}$ ratio decreases linearly at increasing IDR/IDR_u . Note that this approach is consistent with the proposal of Fardis in section 3.5 of [23].

$$\frac{d_{u,dam}}{d_{u,undam}} = 1 - \frac{IDR}{IDR_u} \quad (6)$$

IP load bearing capacity reduction due to OOP displacements was reconstructed based on Flanagan and Bennett's [24] combined IP-OOP test performed on specimen 23. Based on these experimental evidences, if the infill has been damaged by the OOP action represented by the OOP maximum displacement d_{OOP} , the IP force that produces the IP displacement d_{IP} , $F_{IP,dam}(d_{IP}, d_{OOP})$ can be expressed through a simplified linear relationship as:

$$\frac{F_{IP,dam}(d_{IP}, d_{OOP})}{F_{IP,undam}(d_{IP})} = 1 - \frac{d_{OOP}}{d_{OOP,u}} \quad (7)$$

in which $F_{IP,undam}(d_{IP})$ is the IP force that produces the IP displacement d_{IP} of the undamaged panel and $d_{OOP,u}$ is the undamaged infill ultimate OOP displacement.

The proposed empirical-based model has been implemented in OpenSEES [25]. First, the OOP force-displacement behaviour relationship should be defined for the undamaged panel through the semi-empirical approach described in this section. Hereafter, the above-defined OOP behaviour relationship will be mentioned as the $IDR=0$ backbone. Then, n IDRs (IDR_i , with $i=1, \dots, n$) should be set as discrete IP damage thresholds. Through the degradation-modelling relationships, it is possible to define n OOP backbones, corresponding to the n IDRs: each one of these curves, which will be mentioned hereafter as $IDR=IDR_i$ backbone, represents the OOP behaviour that the infill will exhibit from the moment the IP IDR demand exceeds the damage threshold represented by IDR_i (see Figure 2).

Integral part of the proposed model is a routine that removes from the structural model the IDR_{i-1} real plastic hinge and the IDR_i auxiliary plastic hinge when the IP IDR exceeds the previously defined damage threshold represented by IDR_i . In this way, as soon as the IDR exceeds IDR_i and as long as the IDR is lower than the successive IP damage threshold IDR_{i+1} , the panel OOP behaviour is defined by the $IDR = IDR_i$ backbone “contained” in the i th real plastic hinge, while the effects of the remaining plastic hinges are still mutually neutralizing. Moreover, if the OOP displacement exceeds the ultimate displacement associated to the $IDR = IDR_i$ backbone, all the elements representative of the infill wall are removed from the structural model. An explanatory version of the removal routine is shown in Figure 4.

```

PRIOR TO THE STRUCTURAL ANALYSIS

for each Infill Wall modeled
  set CF1, a control flag for the element removal, to 0
  for each ZeroLength element (ZL) carrying a "real" OOP backbone
    set IPLD, the value of the IP displacement at which the ZL must be removed
    set CF2, a control flag for the ZL removal, to 0
    set OOPUD, the value of the ultimate OOP displacement associated to the ZL
  end
end

DURING THE STRUCTURAL ANALYSIS, AT EACH STEP CONVERGED

for each Infill Wall modeled
  set IPD to the current in-plane displacement
  set OOPD to the current out-of-plane displacement
  if (element not already removed, i.e., CF1==0)
    if OOPD>OOPUD
      remove the whole infill wall
      set CF1 to 1
    else
      for i that skims each ZL carrying a "real" OOP backbone
        if (the i-th ZL not already removed, i.e., CF2==0)
          if IPD>IPLD
            remove the i-th ZL carrying the "real" OOP backbone
            remove the ZL carrying the i+1-th "auxiliary" OOP backbone
            set CF2 to 1
          end
        end
      end
    end
  end
end
end
end
end

```

Figure 4. Removal routine simplified schema.

The IP strength and stiffness degradation can be controlled through the ratio between the OOP displacement demand and the OOP displacement capacity of the undamaged panel. It can be modelled, together with the whole infill removal due to the attainment of the IP ultimate displacement, through a procedure very similar the one explained in the previous lines for the modelling of the infill OOP behaviour.

4 CASE-STUDY RC BUILDINGS

4.1 RC frames

Hereafter, the design of 2 RC case-study buildings with rectangular plan is presented (Figure 5). The buildings are provided of 5 and 3 bays in the X and Z direction, respectively. All bays spans are 4.5 m long while the inter-storey height is always equal to 3 m. Each building has been designed for gravity and seismic loads by applying the Response Spectrum Analysis method according to EC2 [26] and EC8 [27]. The case-study buildings designed are distinguished for different values of the design PGA at LS (0.15 g and 0.35 g). The materials used for the building design are class C28/35 concrete and reinforcing steel with yielding stress equal to 450 N/mm². The buildings were designed on a stiff and horizontal type A soil. EC8 Type 1 elastic spectrum, which is recommended for high-seismicity zones, was used to

evaluate horizontal seismic actions. A behaviour factor equal to 4.68 was applied to reduce spectral pseudo-accelerations. All designed buildings resulted regular in plan while not regular elevation due to a non-gradual stiffness reduction along their height. $P-\delta$ effects resulted negligible. The longitudinal and transverse reinforcement for beams and columns were determined accordingly to force demands assessed through RSA and by applying capacity design rules. In order to perform non-linear dynamic analyses, the RC elements non-linearity is modelled through a tri-linear moment-chord rotation backbone provided of the cracking point and perfectly plastic after yielding point. These points are determined through a section analysis and by applying the dispositions about yielding chord rotation given by the Annex A of EC8, part 3 [28].

In the following, each case-study building is defined through an acronym, such as 8PX, in which X is the design PGA at LS expressed in $g/100$ (15 or 35).

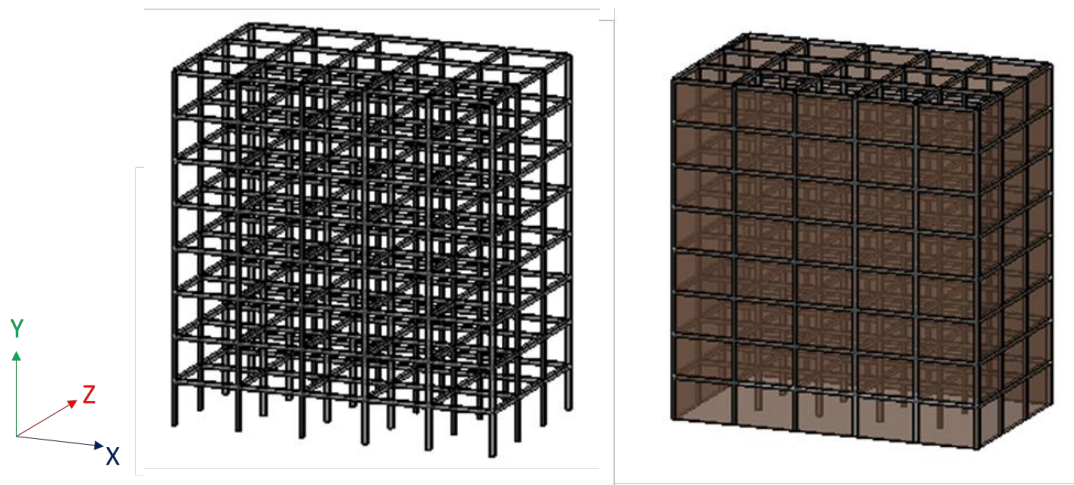


Figure 5. Representation of the bare and infilled case-study buildings.

4.2 Infill walls

A one-leaf 300 mm thick, 4500 wide and 3000 mm high URM infill wall is modelled. Its mechanical properties are the ones calculated for the masonry wallets tested by Guidi et al. [14] (Table 2). The value of the masonry shear strength was set to 0.30 N/mm^2 according to Table 3.4 of EC6 [29].

h/t	m	G [N/mm ²]	τ_{cr} [N/mm ²]	vertical (parallel to holes)		horizontal (perpendicular to holes)	
				E [N/mm ²]	f_m [N/mm ²]	E [N/mm ²]	f_m [N/mm ²]
10	3.3	788	0.30	1767	1.19	4312	6

Table 2. Geometric and mechanical features of the case-study infill.

Each infill wall was introduced in the structural model through a single equivalent strut whose non-linear behaviour is modelled based on Panagiotakos and Fardis proposal [3-4]. The ratio of the softening over the elastic stiffness, α , was set to -3.6%. These assumption lead to predictions of the softening stiffness and ultimate IP displacement in good accordance with the experimental evidences shown by Guidi et al. (specimen URM-U). The OOP behaviour was modelled accordingly to the empirical-based approach discussed in the previous section.

The IP and OOP behaviour characteristic points and the OOP vibration period of the case-study infill, T_a , are reported in Table 3.

IP behaviour			OOP behaviour		
F_{crack}	[kN]	405.0	F_{crack}	[kN]	73.9
K_{crack}	[kN/mm]	354.6	K_{crack}	[kN/mm]	83.9
d_{crack}	[mm]	1.14	d_{crack}	[mm]	0.9
F_{max}	[kN]	526.5	F_{max}	[kN]	281.2
K_{max}	[kN/mm]	40.8	K_{max}	[kN/mm]	63.6
d_{max}	[mm]	12.9	d_{max}	[mm]	4.4
α	[%]	-3.6	d_u	[mm]	16.3
d_u	[mm]	54.1	T_a	[s]	0.035
IDR_u	[%]	1.80			

Table 3. IP and OOP behaviour of the case-study infill.

The infill wall behaviour degradation was modelled through the proposed empirical approach: for instance, the IP degradation was modelled with backbones defined at steps of 0.05 times the $d_{OOP,u}$ displacement while the OOP degradation was modelled with backbones defined at steps of 0.05 times the IDR_u .

The PGA associated to the first OOP collapse (PGA_C) for the case-study buildings assessed through a “code-based approach” on the bare frames, i.e., by matching the infill OOP strength calculated accordingly to EC6 §6.3.2 and the OOP demand acting on them calculated accordingly to EC8 §4.3.5, are reported in Table 5.

	8P15	8P35
PGA_C [g]	0.41	0.38

Table 4. PGA at first OOP infill collapse accordingly to an EC-based approach

5 RECORDS SELECTION FOR INCREMENTAL DYNAMIC ANALYSES AND ANALYSIS PROCEDURE

Seven ground motions were selected among the records of seven different European earthquakes collected in the Engineering Strong-Motion (ESM) Database [30] in order to perform Incremental Dynamic Analyses (IDAs) [31]. Significant characteristics of the selected ground motions are reported in Table 6.

	ESM ID	Country	Date	M	R_{epi} [km]	PGA – NS [g]	PGA – EW [g]
1	ME-1979-0006	Montenegro	15/04/1979	5.8	22.7	0.092	0.080
2	IT-1984-0005	Italy	11/05/1984	5.5	19.2	0.025	0.015
3	IT-1997-0004	Italy	26/09/1997	5.7	24.2	0.023	0.024
4	IT-1998-0103	Italy	09/09/1998	5.6	18.0	0.161	0.156
5	GR-1999-0001	Greece	07/09/1999	5.9	19.7	0.108	0.119
6	TK-1999-0294	Turkey	13/09/1999	5.8	13.8	0.074	0.317
7	IT-2009-0102	Italy	07/04/2009	5.5	15.6	0.131	0.089

Table 5. Selected Ground Motions for Incremental Dynamic Analyses.

The selection of records was performed searching among the bidirectional registration of stations based on EC8 type A soils, consistently with the design soil type. Consistently with the choice of using EC8 Type I design spectrum, only earthquakes with magnitude between 5.5 and 7 and only registration of stations with epicentral distance between 10 and 30 km were considered. The 5%-damped response spectra of the selected records are reported in [Figure 6a](#) (North-South component) and [6b](#) (East-West component). Both horizontal components of the selected records were simultaneously matched to the 5%-damped EC8 design spectrum at LS using wavelets through the RspMatchBi software by Grant [32]. So, two different record-set were defined after matching: a first record-set (R15) used for IDAs on buildings designed for a PGA at LS of 0.15 g, a second record-set (R35) used for IDAs on buildings designed for a PGA at LS of 0.35 g. The response spectra of the R15 and R35 records are shown in [Figure 6c](#) and [6d](#), respectively, together with their mean spectrum and the EC8 target response spectrum.

IDAs were performed by scaling each selected and matched record for a set of pre-determined scale factors in order to obtain for each horizontal direction an incremental PGA (selected as Intensity Measure) vs maximum IDR (selected as Engineering Demand Parameter) curve. Moreover, a bisection procedure was implemented in order to define the PGA associated to the first OOP infill collapse and removal from the structural model with a precision equal to ± 0.01 g. Note that IDAs were performed on a W/ model, in which the degradation of IP and OOP backbones due to interaction was implemented, together with the infill removal routine, and on a W/O model in which only the infill removal routine at the attainment of the IP or OOP collapse displacement was implemented.

The analyses were carried out by applying mass- and tangent stiffness-proportional Rayleigh damping rules for two control vibration modes. A “global” and a “local” mode were selected as control modes. For instance, the first control mode corresponds the first natural frequency of the infilled structure, while the second control mode corresponds to the mode associated to the frequency closer to the infill natural frequency in the OOP direction. The assigned damping ratio is equal to 2% both for the first global and for the second local control mode: the last choice is due to the lack of exhaustive studies on this topic, which is worth to be investigated in the future.

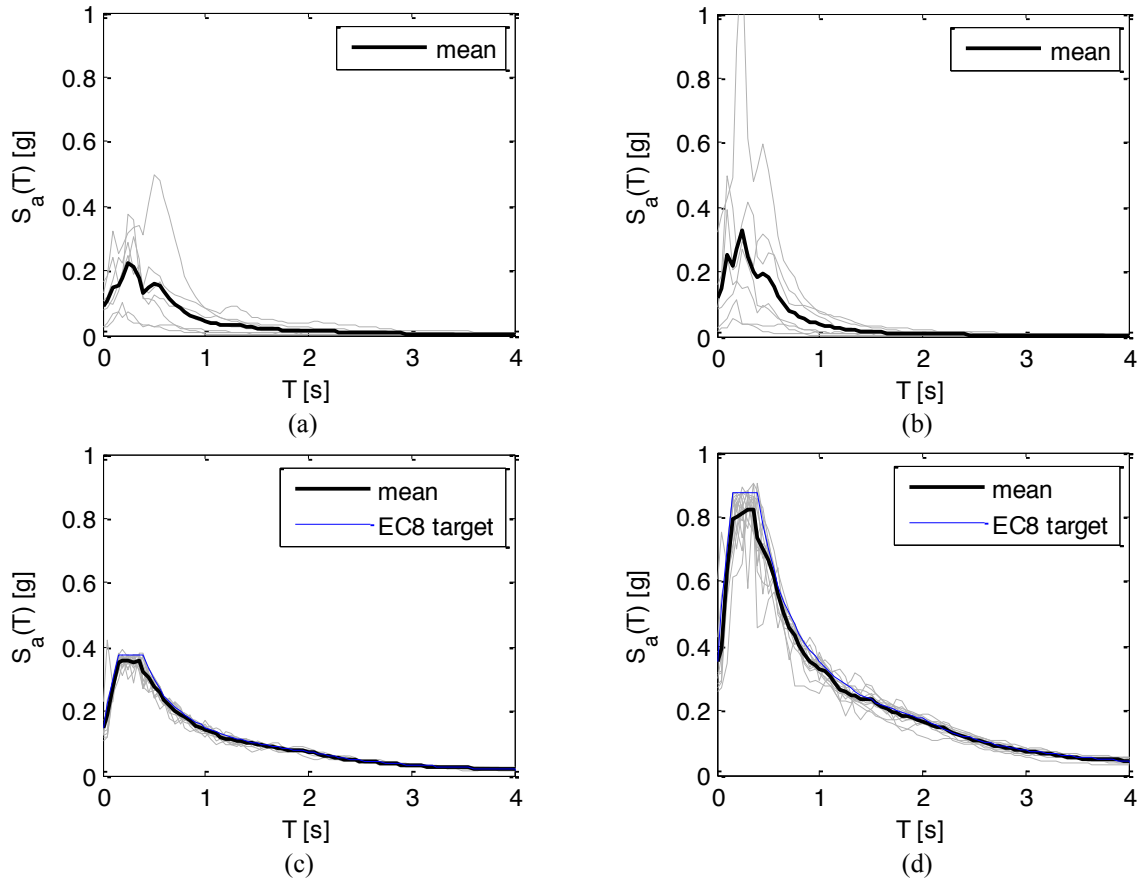


Figure 6. Selected records response spectra for NS component (a), EW component (b). Response spectra of the selected records matched to EC8 design spectrum at LS for PGA=0.15 g (c) and PGA=0.35 g (d).

6 ANALYSES RESULTS

Incremental Dynamic Analyses were performed on the case-study buildings using the OpenSEES software. IDA curves for all case-study buildings are shown for both W/ and W/O models in Figure 7. Median IDA curves for W/ and W/O models are compared in Figure 8.

As expected, IDR demands are greater in the Z direction (less stiff direction of the buildings) and for the W/ model of all case-study buildings. For instance, the maximum IDR demand is underestimated by neglecting IP-OOP interaction especially for buildings designed for a 0.15 g PGA at LS, while building designed for a LS PGA of 0.35 g are provided of structural members with greater inertia properties and are, so, stiffer with respect to horizontal actions. Accounting for IP-OOP interaction seems to be necessary in order to not underestimate displacement demands during seismic analyses.

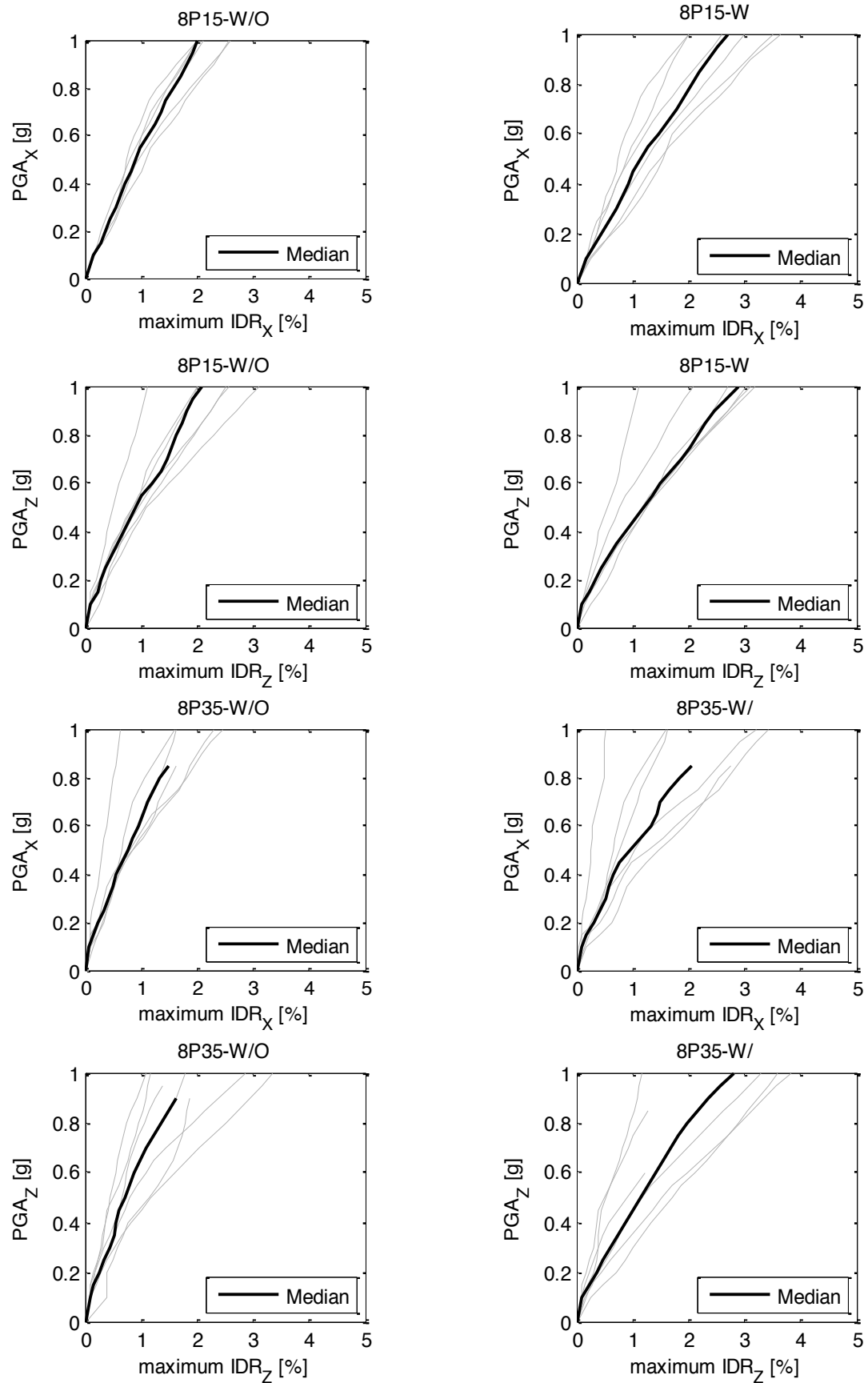


Figure 7. IDA curves for all case-study buildings (grey) together with their median IDA curve (black).

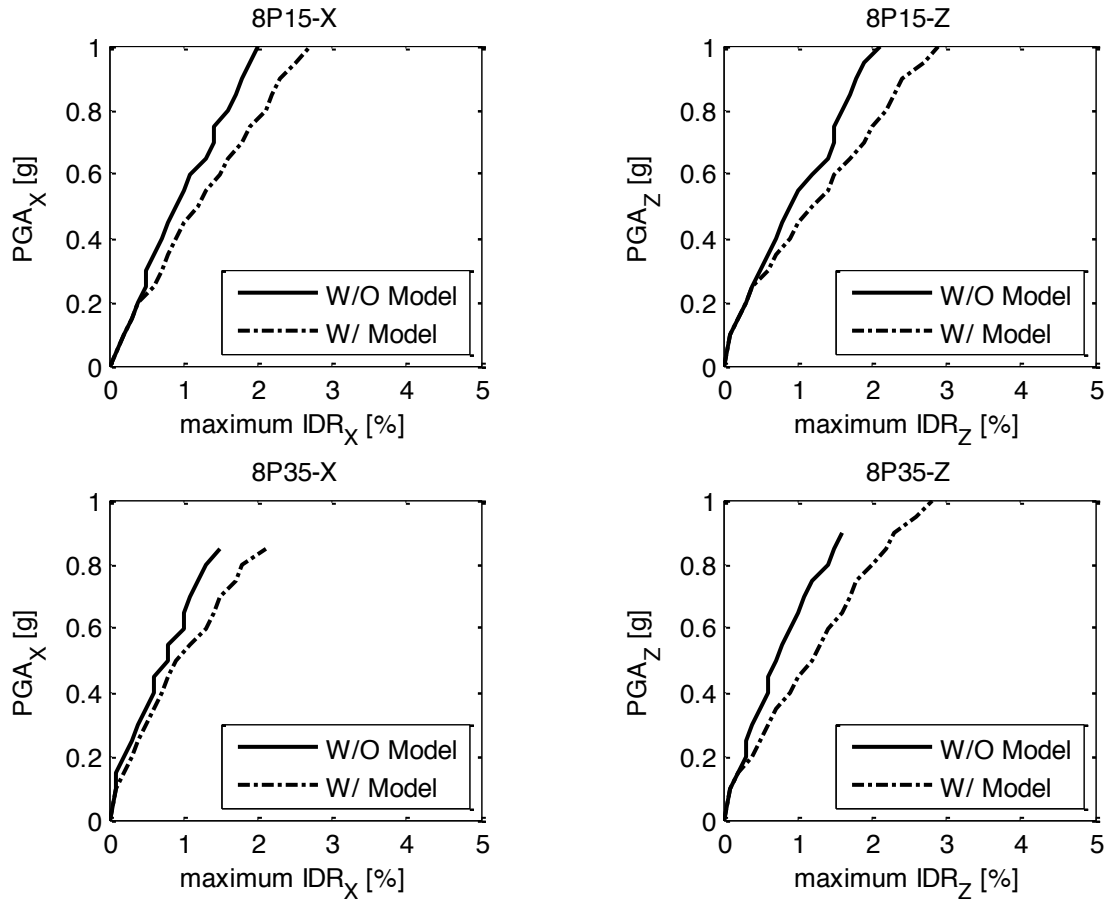


Figure 8. Comparison of median IDA curves for W/O (continuous line) and W/ (dotted line) models of all case-study buildings.

In Table 6, the mean PGA at first OOP collapse for all case-study buildings are reported, together with the lower (L) and higher (H) storey at which the first OOP collapse occurred.

	W/O Model		W/ Model	
	PGA [g]	Storey (L/H)	PGA [g]	Storey (L/H)
8P15	0.28	6/7	0.16	3/4
8P35	0.25	6/8	0.14	3

Table 6. First OOP collapse mean PGA for all case-study buildings.

Generally speaking, they are, as expected, lower for W/ models. In fact, in W/O models the OOP collapse is attained for a fixed OOP collapse displacement equal to 16 mm, while in W/ models the OOP collapse displacement reduces due to IP action. The ratio of the infill natural period in the OOP direction, T_a , over the case-study buildings' vibration period in the same direction, T_1 , is always lower than 1. This means that for stiffer buildings designed for higher PGA at LS, and so provided of lower natural vibration period, the T_a/T_1 ratio is closer to unit than for buildings designed for a lower PGA. For this reason, higher OOP actions are expected for infills in stiffer buildings and so a lower PGA at first OOP collapse is as well expected for buildings designed for a 0.35 g PGA at LS.

Collapse PGAs assessed through dynamic analyses, which accounts for IP-OOP interaction and structural non-linearity, is extremely higher that collapse PGAs evaluated through a code-based approach (Table 4). For instance, the overestimation of OOP collapse PGAs ranges

from 46% (W/O model of 8P15 building) to 132% (W/ model of 8P35 building). Moreover, a code-based approach predicts the first OOP infill collapse at the last storey, while it is expected due to IP-OOP interaction, based on the results of the above described analyses, between the third and the fourth floor. In fact, at intermediate storeys the maximum combined effect of higher IDR demands (increasing from higher to lower storeys) and higher OOP demands (increasing from lower to higher storeys) is expected. Without accounting for IP-OOP interaction, the first OOP collapse is expected at higher storeys (sixth to eighth): in fact, in this case, the OOP collapse is only due to higher OOP demands, which reach their maximum at the higher storeys. Probably, higher modes effects make the maximum OOP demand occur not always at the last storey.

Simplified methods accounting at least for IP-OOP interaction in a linear elastic framework during OOP safety check of infills should be implemented in order to provide an accurate estimate of the OOP collapse PGA, which is often lower than design PGA at LS. Note that at §2.2.2(6)P, EC8 [27] states that at LS: “*it shall be verified that under the design seismic action the behaviour of nonstructural elements does not present risks to persons and does not have a detrimental effect on the response of the structural elements*”. The OOP collapse of infills presents enormous risks for life safety and, in this sense, case-study buildings with first OOP collapse PGA lower than the design PGA (8P35) are not EC8-compliant in the safety check at LS, even if their structural members were designed according to EC8 provisions.

Fragility curves relating the probability of exceeding the DL (maximum IDR demand equal or greater than 0.5%) or the “First OOP Collapse Limit State” (PGA equal to the first OOP collapse PGA) to PGAs for W/ and W/O models are shown in Figure 9.

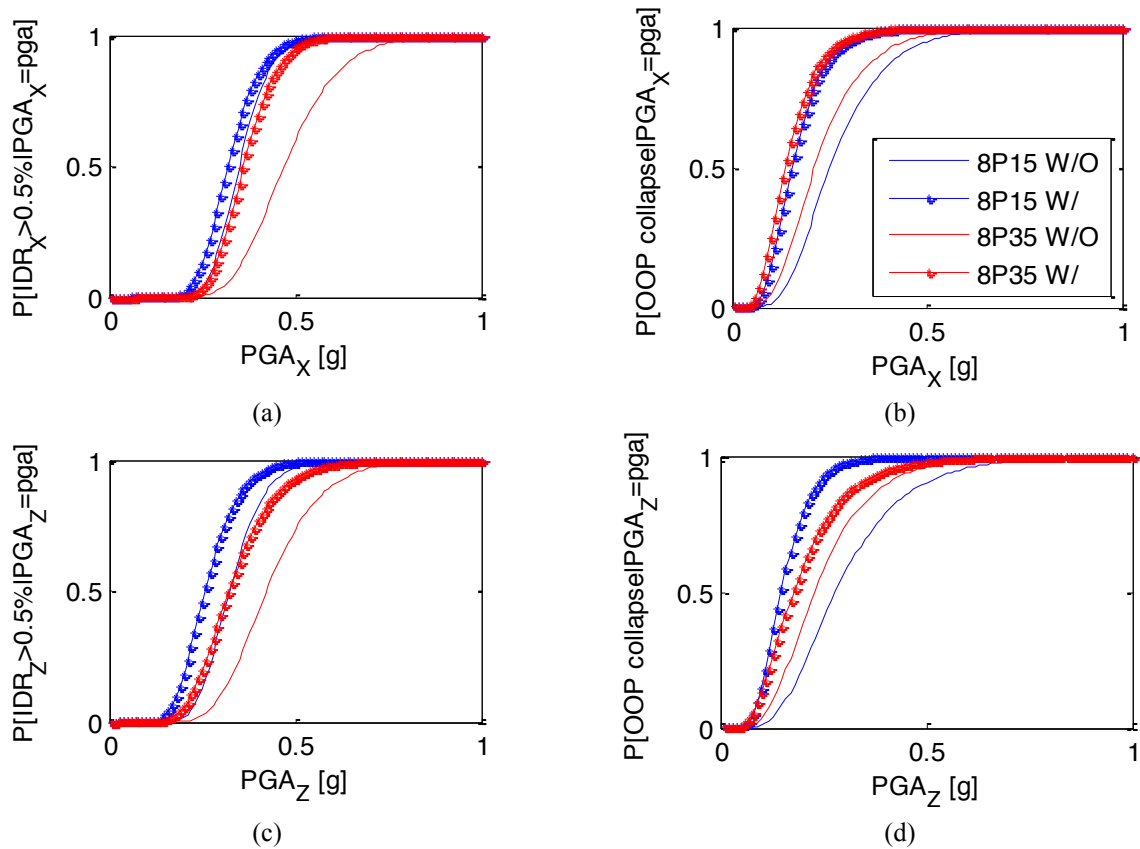


Figure 9. Fragility curves for all case-study buildings in X (a-b) and Z (c-d) directions, with respect to the attainment of DL (a-c) or of the 1st OOP infill collapse (b-d). Legend reported in (b).

First DL exceedance always occurred in the Z direction, while first OOP collapse always involved infills along disposed along Z direction for seismic demand acting along X direction.

Based on the results above discussed in terms of IDA and median IDA curves, the probability of DL exceedance is underestimated for W/O models due to the underestimation of IP displacement demands caused by the effects of OOP demand on the IP infill behaviour, which are neglected if the IP-OOP interaction is neglected. The design at higher PGA at LS produces structural elements with higher inertia properties. For this reason, at equal upper-limit PGA, a noticeably lower probability of DL exceedance is expected and observed for 8P35 case-study building. The probability of OOP collapse activation is, as expected, underestimated for W/O models. Values closer to unit for the ratio of the infill OOP vibration period over the supporting structure vibration period, which lead to a higher dynamic amplification of OOP demands along the building height are expected for stiffer buildings. For this reason, at equal upper-limit PGA, a noticeably higher probability of first OOP occurrence is expected, in general, for stiffer buildings, such as those designed for a higher PGA at LS, and is observed for the 8P35 case-study building.

7 CONCLUSIONS

This research paper is focused on the out-of-plane (OOP) behaviour of URM infills walls and on the effects on it of the in-plane (IP) displacement demand and vice-versa, i.e., the IP-OOP interaction effects. Modelling infills accounting for their OOP behaviour and for the IP-OOP interaction is the main topic of this work. For instance, Incremental Dynamic Analyses were carried out on two Eurocodes-conforming 8-storeys RC buildings designed for two different PGA acceleration at Life Safety Limit State (0.15 and 0.35 g), in order to analyze the effects of taking or not taking account of the IP-OOP interaction effects in the case-study buildings seismic assessment.

First, a state-of-the-art on the OOP infills behaviour and on the IP-OOP interaction modelling is presented. Then, a novel empirical-based model for URM infills accounting for OOP behaviour and IP-OOP interaction implemented in OpenSEES is presented. The proposed model is applied to model the thick infills of the case-study buildings, whose characteristics are briefly described. 7 bidirectional ground motions were selected among the records of strong European records. The ground motion components were simultaneously matched to the design spectrum at Life Safety Limit State (LS) of the case-study buildings. IDA curves for all records, their median curve and fragility curves with respect to the attainment of Damage Limitation Limit State (DL) and of the first OOP infill collapse are shown to summarize dynamic analyses' results, together with the mean of PGAs at first OOP collapse assessed during analyses for all case-study buildings.

The analyses results showed that the IP displacement demand is noticeably underestimated if the IP-OOP interaction is neglected, especially for buildings designed for lower PGA at LS and so constituted of structural members provided of low inertial properties. If IP-OOP interaction is neglected, the probability of DL exceedance is underestimated for all PGA demands. PGA associated to the first OOP collapse is underestimated if IP-OOP interaction is neglected, especially for stiffer buildings designed for higher PGA at LS. Moreover, an EC-based approach in assessing the PGA associated to the first infill OOP collapse could overestimate that PGA up to 132%. In order to not overestimate RC buildings' performances with respect to both DL and LS Limit States, IP-OOP interaction modelling seems unavoidable.

In future works, further analyses should be carried out involving a greater number of case-study buildings, different for number of storeys and design PGAs. Different infills' layout should be also considered. Simplified methods aimed at assessing the OOP capacity of infills accounting for IP-OOP interaction phenomena in a code-based framework should be defined.

ACKNOWLEDGEMENTS

This work was developed under the financial support of METROPOLIS (*Metodologie e tecnologie integrate e sostenibili per l'adattamento e la sicurezza di sistemi urbani - PON Ricerca e Competitività 2007-2013*) and ReLUIS-DPC 2014-2018 Linea Speciale RS12 *Tamponature*, funded by the Italian Department of Civil Protection (DPC). These supports are gratefully acknowledged.

REFERENCES

- [1] A. Filiatrault, T. Sullivan, Performance-based seismic design of nonstructural building components: The next frontier of earthquake engineering. *Earthquake Engineering and Engineering Vibration*, **13.1**, 17-46, 2014.
- [2] S. Taghavi, E. Miranda, Seismic performance and loss assessment of nonstructural building components. *Proceedings of 7th National Conference on Earthquake Engineering*, Boston, United States of America, July 21-25, 2002.
- [3] M.N. Fardis, T.B. Panagiotakos, Seismic design and response of bare and masonry-infilled reinforced concrete buildings. Part II: infilled structures. *Journal of Earthquake Engineering*, **1.3**, 475-503, 1997.
- [4] T.B. Panagiotakos, M.N. Fardis, Seismic response of infilled RC frames structures. *11th World Conference on Earthquake Engineering*, Acapulco, Mexico, June 23-28, 1996.
- [5] A. Saneinejad, B. Hobbs, Inelastic design of infilled frames. *Journal of Structural Engineering*, **121.4**, 634-650, 1995.
- [6] R.J. Mainstone, On the stiffness and strength of infilled frames. *Proc., Supplement (IV), Paper 7360S, Instn. of Civ. Engrs.*, London, England, 1971.
- [7] E.L. McDowell, K.E. McKee, E. Sevin, Arching action theory of masonry walls. *Journal of the Structural Division*, **82.2**, 1-8, 1956.
- [8] R. Angel, D.P. Abrams, D. Shapiro et al., *Behaviour of reinforced concrete frames with masonry infills*. University of Illinois Engineering Experiment Station. College of Engineering. University of Illinois at Urbana-Champaign., 1994.
- [9] J.L. Dawe, C.K. Seah, Out-of-plane resistance of concrete masonry infilled panels. *Canadian Journal of Civil Engineering*, **16.6**, 854-864, 1989.
- [10] R.D. Flanagan, R.M. Bennett, Arching of masonry infilled frames: Comparison of analytical methods. *Practice Periodical on Structural Design and Construction*, **4.3**, 105-110, 1999.
- [11] S. Kadysiewski, K.M. Mosalam, *Modelling of unreinforced masonry infill walls considering in-plane and out-of-plane interaction*. Pacific Earthquake Engineering Research Center, 2009.
- [12] M.C. Griffith, J. Vaculik, N.T.K. Lam et al., Cyclic testing of unreinforced masonry walls in two-way bending. *Earthquake Engineering & Structural Dynamics*, **36.6**, 801-821, 2007.
- [13] G.M. Calvi, D. Bolognini, Seismic response of reinforced concrete frames infilled with weakly reinforced masonry panels. *Journal of Earthquake Engineering*, **5.2**, 153-185, 2001.

- [14] G. Guidi, F. da Porto, M. Dalla Benetta et al., Comportamento sperimentale nel piano e fuori piano di tamponamenti in muratura armata e rinforzata. *Proceedings of the XV ANIDIS, L'Ingegneria Sismica in Italia*, Padua, Italy, June 30 – July 4, 2013 (in Italian).
- [15] A. Furtado, H. Rodrigues, A. Arêde, H. Varum, Experimental evaluation of out-of-plane capacity of masonry infill walls. *Engineering Structures*, **111**, 48-63, 2016.
- [16] S.A. Hashemi, K.M. Mosalam, *Seismic evaluation of reinforced concrete buildings including effects of infill masonry walls*. Pacific Earthquake Engineering Research Center, 2007.
- [17] A. Furtado, H. Rodrigues, A. Arede, H. Varum, Simplified macro-model for infill masonry walls considering the out-of-plane behaviour. *Earthquake Engineering & Structural Dynamics*, **45.4**, 507-524, 2015. DOI: 10.1002/eqe.2663.
- [18] F. Longo, G. Granello, G. Tecchio, F. da Porto, C. Modena, A masonry infill wall model with in-plane out-of-plane interaction applied to pushover analysis of RC frames. *Brick and Block Masonry: Proceedings of the 16th International Brick and Block Masonry Conference*, Padua, Italy, June 26-30, 2016.
- [19] P.B. Shing, L. Cavaleri, F. Di Trapani, Prediction of the out-of-plane response of infilled frames under seismic loads by a new fiber-section macro-model. *Brick and Block Masonry: Proceedings of the 16th International Brick and Block Masonry Conference*, Padua, Italy, June 26-30, 2016.
- [20] M. Oliace, G. Magenes, In-plane out-of-plane interaction in the seismic response of masonry infills in RC frames. *Brick and Block Masonry: Proceedings of the 16th International Brick and Block Masonry Conference*, Padua, Italy, June 26-30, 2016.
- [21] M. Di Domenico, P. Ricci, G.M. Verderame, Empirical unreinforced masonry infill macro-model accounting for in-plane/out-of-plane interaction. *COMPDYN 2017*, Rhodes Island, Greece, June 15-17, 2017.
- [22] S.P. Timoshenko, S. Woinowsky Krieger, *Theory of plates and shells*. McGraw-Hill, New York, 1959.
- [23] M.N. Fardis (editor), *Experimental and numerical investigations on the seismic response of RC infilled frames and recommendations for code provisions, ECOEST/PREC8 Report No.6*, Laboratorio Nacional de Engenharia Civil Publications, Lisbon, 1996.
- [24] R.D. Flanagan, R.M. Bennett, Bidirectional behaviour of structural clay tile infilled frames. *Journal of Structural Engineering*, **125.3**, 236-244, 1999.
- [25] F. McKenna, G.L. Fenves, M.H. Scott, *Open system for earthquake engineering simulation*. University of California, Berkeley, CA, 2000.
- [26] Eurocode 2 (ENV 1992-1-1). Design of concrete structures. 1: General rules and rules for buildings, Brussels, 2004.
- [27] Eurocode 8 (ENV 1998-1-1). Design provisions for earthquake resistance of structures. Brussels, Belgium: European Committee for Standardization, 2003.
- [28] Eurocode 8 (ENV 1998-3). Design provisions for earthquake resistance of structures. Brussels, Belgium: European Committee for Standardization, 2003.

- [29] EN 1996-1-1 Eurocode 6: Design of masonry structures - Part 1-1: General rules for reinforced and unreinforced masonry structures, 2005.
- [30] L. Luzi, R. Puglia, E. Russo, ORFEUS WG5, Engineering Strong Motion Database, version 1.0. Istituto Nazionale di Geofisica e Vulcanologia, Observatories and Research Facilities for European Seismology. DOI: 10.13127/ESM.
- [31] D. Vamvatsikos, C.A. Cornell, Incremental dynamic analysis. *Earthquake Engineering and Structural Dynamics*, **31.3**, 491-514, 2002.
- [32] D.N. Grant, Response spectral matching of two horizontal ground-motion components. *Journal of Structural Engineering*, **137.3**, 289-297, 2010.